Neuron, Vol. 46, 219–232, April 21, 2005, Copyright ©2005 by Elsevier Inc. DOI 10.1016/j.neuron.2005.02.029

Mutations in *Drosophila sec15* Reveal a Function in Neuronal Targeting for a Subset of Exocyst Components

Sunil Q. Mehta,[1,6] P. Robin Hiesinger,[2,6] Slobodan Beronja,[5] R. Grace Zhai,[2] Karen L. Schulze,[2] Patrik Verstreken,[3] Yu Cao,[3] Yi Zhou,[3] Ulrich Tepass,[5] Michael C. Crair,[1,4] and Hugo J. Bellen[1,2,3,4,*]

[1]Program in Developmental Biology
[2]Howard Hughes Medical Institute
[3]Department of Molecular and Human Genetics
[4]Department of Neuroscience
Baylor College of Medicine
One Baylor Plaza
Houston, Texas 77030
[5]Department of Zoology
University of Toronto
Toronto, Ontario M5S 3G5
Canada

Summary

The exocyst is a complex of proteins originally identified in yeast that has been implicated in polarized secretion. Components of the exocyst have been implicated in neurite outgrowth, cell polarity, and cell viability. We have isolated an exocyst component, *sec15*, in a screen for genes required for synaptic specificity. Loss of *sec15* causes a targeting defect of photoreceptors that coincides with mislocalization of specific cell adhesion and signaling molecules. Additionally, *sec15* mutant neurons fail to localize other exocyst members like Sec5 and Sec8, but not Sec6, to neuronal terminals. However, loss of *sec15* does not cause cell lethality in contrast to loss of *sec5* or *sec6*. Our data suggest a role of Sec15 in an exocyst-like subcomplex for the targeting and subcellular distribution of specific proteins. The data also show that functions of other exocyst components persist in the absence of *sec15*, suggesting that different exocyst components have separable functions.

Introduction

Twenty-five years ago, Novick et al. (1980) identified 23 temperature-sensitive mutant complementation groups that caused a secretory defect in yeast. Many of the *SEC* mutants isolated in this work have now been studied in more detail (Schekman and Novick, 2004). Much is known about some of these genes, including *SEC9*, a SNAP-25 homolog, *SEC17*, an α-SNAP homolog, and *SEC18*, an NSF homolog, because they have been implicated in numerous secretory processes in yeast and many metazoans (Bennett and Scheller, 1993). Another subset of *SEC* genes (*SEC3*, *SEC5*, *SEC6*, *SEC8*, *SEC10,* and *SEC15*) has been shown to encode members of a large protein complex, the exocyst or Sec6/8 complex, which also includes Exo70p and Exo84p. Although they have been studied quite extensively in yeast (Hsu et al., 2004; TerBush et al., 1996), their role in metazoans is ill-defined due to a dearth of functional studies.

In yeast, exocyst proteins are required for polarized exocytosis of secretory vesicles (Guo et al., 1999; TerBush et al., 1996). Sec3p localizes to the membrane even when other exocyst members are lacking and is thought to represent a spatial landmark (Finger and Novick, 1998). Sec15p interacts with the secretory vesicle-associated rab GTPase, Sec4p, in its GTP bound form. A further interaction of Sec15p with Sec10p is thought to recruit other exocyst components and connect the complex to Sec3p (Guo et al., 1999). Hence, Sec15p is thought to target the vesicle to the correct exocytic site.

In multicellular organisms, the exocyst proteins were found to be present in brain (Guo et al., 1999; Hsu et al., 1996) as well as most other tissues (Hsu et al., 1999; Kee et al., 1997). In nonpolarized epithelial cells (Madin-Darby canine kidney [MDCK] cell culture), the complex is found in a soluble form in the cytoplasm. Upon cell-cell contact, it relocalizes to the interacting plasma membranes. After disruption of E-cadherin-mediated cell-cell contact, the complex dissociates again from the plasma membrane. In the same epithelial cell line, antibodies against Sec8 specifically inhibited vesicle delivery to the basolateral but not the apical membrane (Grindstaff et al., 1998; Yeaman et al., 2004). These data suggest that the recruitment of the exocyst is a consequence of cell-cell adhesion and is essential for epithelial cell polarity.

In cultured hippocampal neurons, Sec6 immunoreactivity is present in the growth cone during neurite outgrowth as well as in periodic punctae on the axon prior to synaptogenesis. After formation of stable synapses, the Sec6 immunoreactivity disappears, suggesting that Sec6 protein and the corresponding complex are not required in mature synapses (Hazuka et al., 1999). In addition, overexpression of a dominant-negative Sec10 protein blocks neurite outgrowth in cultured PC12 cells (Vega and Hsu, 2001). Taken together, the data from yeast and mammalian cells suggest that the complex may play a role in growth cone extension and possibly synaptogenesis (Hsu et al., 1999).

To date, the only published mutants providing in vivo data in metazoans are knockouts of *sec8* in mouse and *sec5* in *Drosophila*. The *sec8* knockout results in lethality at E7.5, precluding analyses of neuronal development (Friedrich et al., 1997). Loss of *sec5* in *Drosophila* reveals no defect in neurotransmitter release, and larvae die soon after their maternal protein contribution is exhausted (Murthy et al., 2003). In cell culture, loss of *sec5* blocks neurite outgrowth and incorporation of newly synthesized transmembrane proteins into the membrane, in agreement with a proposed role for the exocyst in neurite outgrowth (Hsu et al., 1999; Murthy et al., 2003). In the developing oocyte, *sec5* is required for membrane trafficking and polarization (Murthy and Schwarz, 2004). Finally, clones of *sec5* in the eye do

*Correspondence: hbellen@bcm.tmc.edu
[6]These authors contributed equally to this work.

not form eye tissue. Since Sec5 is a core component of the complex, Murthy et al. (2003) propose that the phenotype associated with the loss of *sec5* represents the function of the entire exocyst complex. No functional data in yeast or metazoans so far indicate any role of individual exocyst components independent of the entire complex, suggesting that *sec5* mutant phenotypes represent a generic consequence of mutations in exocyst members.

Here, we describe the isolation of *Drosophila sec15* mutants in a forward genetic screen designed to identify genes that affect synapse development. In contrast to the cell lethality associated with *sec5* mutations, *sec15* mutant photoreceptor neurons are viable and display surprisingly specific defects in a distinct neuronal targeting step. Loss of *sec15* does not cause defects in neurite extension, but leads to the formation of synapses between inappropriate partners, causing a loss of synaptic specificity. Our data indicate that *sec15* is required for the delivery of specific cell adhesion and signaling molecules required for the establishment of synaptic specificity after the growth cones reach their target regions. They also suggest a model in which subcomplexes of the exocyst perform separable functions.

Results

Isolation of Mutations in Complementation Group *3R41*

To isolate new genes that play a role in synapse development or function, we carried out an F1 screen in the *Drosophila* visual system (Verstreken et al., 2003). Using the *eyFLP* system, we created 210,000 flies with eyes homozygous for a randomly induced chemical mutation while the rest of the body is heterozygous (Newsome et al., 2000; Stowers and Schwarz, 1999; Verstreken et al., 2003). As shown in Figure 1A, we employed two assays to identify mutations that cause a failure to evoke a postsynaptic response. To identify mutations that affect the accuracy of synaptic contacts (synaptic specificity), we assessed neuronal targeting defects with light microscopy for 450 mutants and synapse formation with electron microscopy for 40 complementation groups (Figure 1A).

We selected flies with grossly normal eye morphology that phototax poorly or not at all (Benzer, 1967). As shown in Figure 1B, control flies (black) consistently walk toward light, while flies that do not synthesize the neurotransmitter histamine (green) fail to phototax (Burg et al., 1993). Two independently isolated mutations that failed to complement each other (see below), $3R41^{1}$ and $3R41^{2}$, display an aberrant response to light (red and blue). We performed electroretinograms (ERGs) to identify mutations that cause a lack of "on" and "off" responses (Figure 1C, arrows) but display a normal depolarization profile. The lack of an on and off response is thought to indicate a lack of, or aberrant communication between, pre- and postsynaptic cells. This can be caused by (1) a defect in neurotransmission or (2) a developmental defect in synapse formation. To test for developmental defects at the level of light microscopy, we stained adult brains with the photoreceptor-specific antibody against chaoptin, mAb 24B10 (Fujita et al., 1982). The *Drosophila* compound eye consists of 800 unit eyes, called ommatidia, each with a complement of eight photoreceptor cells. mAb 24B10 staining reveals the morphology of photoreceptor terminals R1–R6 in the first optic neuropil, the lamina, as well as R7–R8 in the second optic neuropil, the medulla (Figure 1D). 3D visualization of the R7/8 terminal field in the medulla of a control animal reveals a highly regular array of terminals (Figure 1E). The terminals of R7 and R8 synapse in separate layers in the medulla (Fischbach and Dittrich, 1989; Figure1F). In contrast, $3R41^{1}$ mutant photoreceptors display loss of the regular array of terminals in the medulla (Figure 1G) and highly aberrant R7 and R8 target layering (Figure 1H). We next analyzed whether these morphological disruptions are the result of long-range growth cone guidance defects or short-range wiring disruptions within the correct brain areas. Visualization of the adult optic neuropils with the synaptic marker N-cadherin revealed strong morphological disruptions of neuropil shape, but no alteration of their arrangement or size, indicating morphological disruptions only within the neuropils (Figures S1A and S1B in the Supplemental Data available with this article online) in mutant optic lobes. Visualization of only the R7 photoreceptor using R7-specific GFP expression (Lee et al., 2001) in an *eyFLP 3R41* mutant background revealed that all observable R7 terminals project into the distal medulla (Figures S1C–S1G). While gross defects in R7 axon outgrowth were not detected, we cannot rule out more subtle defects that are beyond the resolution of the analyses described here. However, our data indicate that axons are not affected in long-range axonal pathfinding, axon extension, and the recognition of the correct brain areas or neuropils. Based on our ERG results, mutant photoreceptors are able to sense light and depolarize normally after stimulation. Taken together, these data suggest that 3R41 mutant neurons do not exhibit disruptions in general cellular processes, but exhibit a severe and specific defect of neuronal terminals in establishing a normal, local wiring pattern within their correct neuropils.

Mutations in *3R41* Cause Defects in Synaptic Specificity

To determine whether R1–R6 photoreceptors display defects in synapse morphology, synapse formation, or vesicle morphology/number, we analyzed wild-type and mutant laminae by transmission electron microscopy (TEM). R1–R6 terminals from different ommatidia are organized into synaptic units called cartridges (Figure 1D). During late larval stages, axons of R1–R6 invade the developing lamina plexus, where their growth cones are halted by interactions with glial cells (Poeck et al., 2001; Figure 2A). Initially, photoreceptors from the same ommatidium travel together in bundles. Later, during the first half of pupation, the R1–R6 terminals defasciculate and organize themselves into cartridges. In this sorting process, photoreceptors that receive light from the same point in space but reside in different ommatidia sort into a single cartridge according to the principle of neural superposition (Clandinin and Zipursky, 2000; Kirschfeld, 1967). Synaptogenesis does not start before cartridge formation is complete at the be-

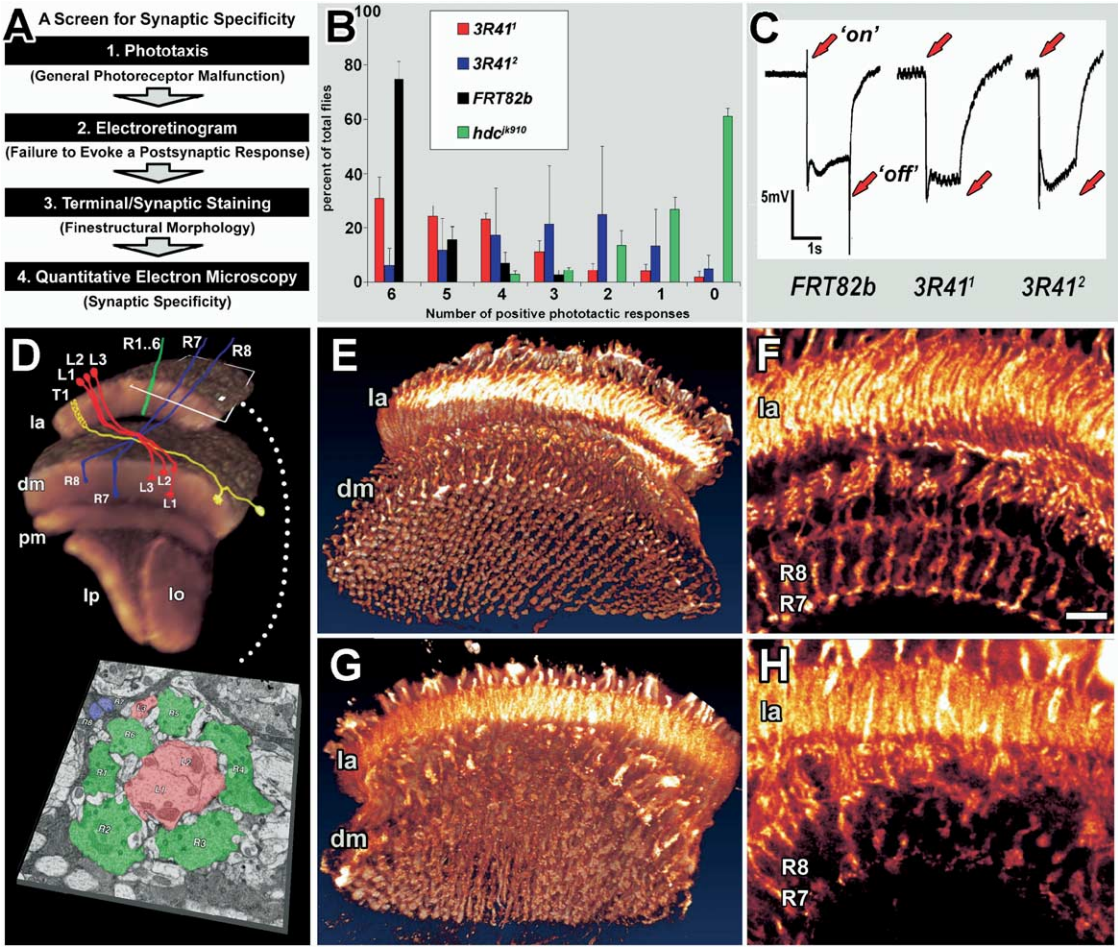

Figure 1. Isolation of 3R41 Mutations in an *eyFLP* Screen

(A) Flowchart of the four sequential assays used to identify mutations affecting synaptic specificity. (B) Comparison of performance of wild-type (*eyFLP; FRT82B*, black), *3R41* mutants (*eyFLP; 3R41^{1,2}/FRT82B cl*, red and blue), and neurotransmitter-deficient (*hdc^{ik910}*, green) flies in the countercurrent phototaxis assay. n = 5 trials with 100 flies per trial. Error bars indicate standard error. (C) Electroretinogram traces from wild-type and mutant flies. Notice that mutants have normal depolarization in response to light, but lack on and off transients (red arrows). (D) Illustration of selected neuronal projections in the adult optic lobe (upper panel). The lower panel shows an ultrathin cross-section of a cartridge in the lamina. Neuronal projections in both panels are color coded with the presynaptic photoreceptors R1–R6 in green and the postsynaptic lamina monopolars L1–L3 in red. Photoreceptors R7–R8 (blue) project through the lamina into the second optic neuropil medulla. la, lamina; dm, distal medulla; pm, proximal medulla; lp, lobula plate; lo, lobula. (E) 3D visualization of the R7/8 terminal field viewed from inside the brain. The confocal image stack was obtained from an *eyFLP FRT82B* control optic lobe stained with mAb24B10. (F) Single optical section of stack used in (E) illustrating R7 and R8 terminal layers in the medulla. (G) 3D visualization of a confocal image stack taken of an adult *eyFLP 3R41^{1}* mutant optic lobe, as in (E). (H) Single optical section of stack used in (G) illustrating the lack of distinct R7/R8 terminal layering in a *3R41^{1}* mutant medulla. Scale bar for (F) and (H) in (F), 10 μm.

ginning of the second half of pupation (Meinertzhagen and Hanson, 1993). We performed quantitative ultrastructural studies of 1-day-old adults to assess cartridge formation and synapse formation. As shown schematically in Figure 1D as well as the control in Figure 2B, cartridges consist of six photoreceptor terminals that surround the processes of the L1 and L2 postsynaptic lamina monopolar cells. Photoreceptor terminals were identified based on the presence of capitate projections (Meinertzhagen and Hanson, 1993). The cartridges are delimited by epithelial glia. In *eyFLP; 3R41^{1}* and *eyFLP; 3R41^{2}* mutant laminae, cartridges are easily identifiable, but they contain highly variable numbers of photoreceptor terminals (Figures 2C and 2D). Quantitative analysis of terminal number per cartridge revealed that *eyFLP; 3R41* mutant laminae have a much broader distribution of photoreceptor terminals per cartridge than wild-type (Figure 2D, see figure legend), indicating a defect in cartridge formation.

Next we analyzed whether synapses are formed in these mis-sorted cartridges. *Drosophila* photoreceptors form tetrad synapses in which the presynaptic active zone makes contacts with four postsynaptic dendrites from lamina monopolar and amacrine cells (Frohlich and Meinertzhagen, 1983). As shown in Figure 2E, the presynaptic active zone is identified by an electron-dense structure known as the "T bar" (Frohlich and Meinertzhagen, 1983; Stark et al., 1989) (Figures 2E

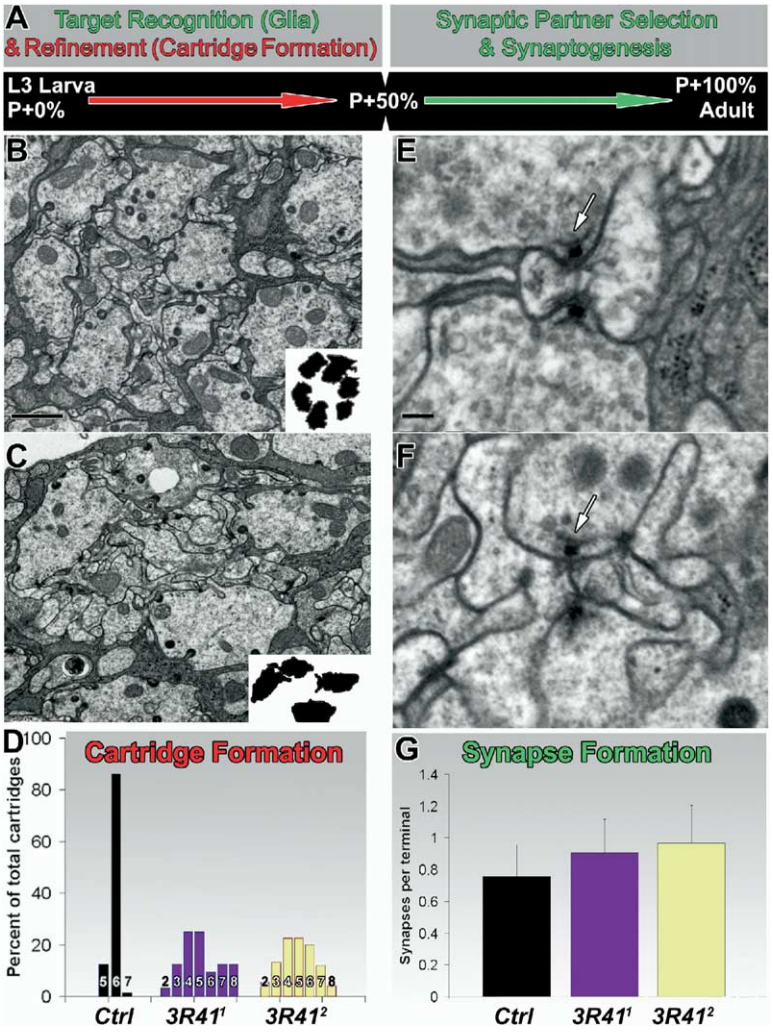

Figure 2. Mutations in *3R41* Cause Defects in Synaptic Specificity

(A) Timeline of lamina development. Note that target recognition and cartridge formation occur before synapse formation. Largely unaffected developmental steps in *3R41* mutants based on adult ultrastructure are depicted in green; the disrupted process of cartridge formation is depicted in red. (B) TEM of a cartridge from a control (*eyFLP; FRT82B*) lamina with the inset showing outlines of the six photoreceptor terminals in the cartridge (compare to Figure 1D). (C) TEM of a cartridge from a mutant (*eyFLP; FRT 3R41¹/FRT82B cl*) lamina with the inset showing the outlines of the four photoreceptor terminals in the cartridge. (D) Distribution of photoreceptor terminals per cartridge for wild-type (black, n = 129 cartridges from 6 flies) and mutant (purple, *3R41*^{1}, n = 75 cartridges from 5 flies; and yellow, *3R41*^{2}, n = 32 cartridges from 3 flies) laminae. Notice that mutant laminae have a much broader distribution of terminals per cartridge than wild-type, revealing a significant defect in cartridge formation (*3R41*^{1} distribution F test = 4.911×10^{-42}; *3R41*^{2} distribution F test = 2.559×10^{-37}). (E) TEM of synapses in photoreceptor terminals in a wild-type lamina. Presynaptic sites of release are marked by the presence of "T bars" (arrows in [E] and [F]), postsynaptic sites are split and marked by densities. (F) TEM of synapses in photoreceptors in a *3R41*^{1} mutant lamina. Notice there is no morphological difference between the synapse structure in (E) and (F). (G) Quantification of average number of synapses per photoreceptor terminal in wild-type (black, 0.76; n = 760 terminals) and mutant (purple, *3R41*^{1}, 0.90, n = 368; and yellow, *3R41*^{2}, 0.97, n = 164). Error bars shown are standard deviations. Scale bar for (B) and (C) in (B), 1 μm. Scale bar for (E) and (F) in (E), 100 nm.

and 2F, arrows), and at least two of the four postsynaptic dendrites are identifiable in an ultrathin section at most angles. We observed the typical configuration of tetrad synapses in which two T bars face each other and share postsynaptic processes (Figure 2F). In *eyFLP; 3R41* mutant laminae, synapses appear morphologically normal and occur with a similar frequency as in controls (Figures 2E–2G), indicating that *3R41* mutants have no defect in synapse assembly. The synaptic vesicle content of mutant terminals appears to be normal, and immunohistochemical analyses of synaptic vesicle proteins including synaptotagmin and neuronal synaptobrevin revealed no altered distribution (data not shown). We conclude that *3R41* mutants exhibit a defect in synaptic specificity, since qualitatively and quantitatively normal synapses are formed in cartridges containing an incorrect complement of photoreceptor terminals.

Homozygous mutant *eyFLP; 3R41* eyes are generally smooth with only occasional irregularities in the ommatidial array (Figure S2A). To ensure that the observed defects are not due to secondary defects in photoreceptor specification or differentiation, we labeled third instar larval imaginal discs containing marked *3R41* mutant clones at the time of axonal outgrowth with a variety of markers. We did not observe any obvious defects in patterning (Figure S2). Since early developing mutant photoreceptors are indistinguishable from wild-type and photoreceptors are able to respond to light stimuli (as evidenced by normal depolarization of the ERG), we conclude that the targeting defects are not due to neuronal differentiation defects.

3R41 Corresponds to *Drosophila sec15*

To identify the molecular lesions that underlie the phenotypes associated with complementation group *3R41*, we performed complementation analysis using deficiencies of chromosome 3R (Figure 3A). Noncomplementation with *Df(3R)e-R1* (93B6;93D2) and complementation with *Df(3R)e-N19* (93B8;94A8) define an ~50 kb region (Figure 3A). We used temperature gradient capillary electrophoresis to screen this 50 kb interval for point mutations (Zhai et al., 2003) and sequenced candidate genes. We identified two premature stop codons in *sec15* at amino acid 135 (*3R41*^{1}) and 226 (*3R41*^{2}), and we renamed *3R41*^{1} as *sec15*^{1} and *3R41*^{2} as *sec15*^{2}

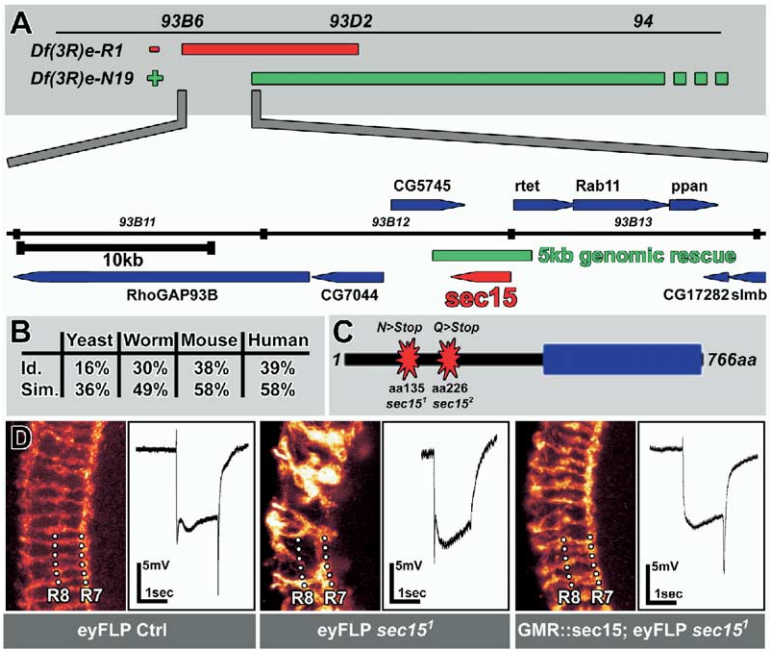

Figure 3. Identification of Mutations in *sec15*

(A) Schematic showing the overlapping deficiencies used to identify the genomic region containing the *3R41* mutations. The lower part of the panel shows genes in the region identified by the deficiencies as well as the genomic rescue construct for *sec15*.

(B) Conservation of Sec15 homologs across species. Values in the table refer to identity and similarity of each homolog when compared to *Drosophila* Sec15.

(C) Schematic of the Sec15 protein showing locations of the stop codons in *3R41*^{1} and *3R41*^{2}. Blue box indicates fragment used to make the Sec15 antibody used in Figure 4.

(D) Photoreceptor-specific expression of *sec15* cDNA using *GMR-Gal4* in an *eyFLP* mutant background rescues the R7/R8 layering as well as ERG defects of *3R41* mutants.

(Figure 3). Both alleles in all transheterozygous combinations with deficiencies die as second instar larvae, indicating that *sec15*^{1} and *sec15*^{2} are either strong hypomorphs or null alleles of *sec15.* Western blot analysis with a polyclonal antibody against the full-length protein did not reveal detectable amounts of protein (see Experimental Procedures) in mutants. RT-PCR using a primer set to detect the truncated RNAs revealed reduced RNA levels, suggesting nonsense-mediated decay of the truncated RNAs (data not shown).

Sec15 is conserved from yeast to humans over the length of the protein (Figure 3B). We were able to rescue the second instar lethality associated with the loss of *sec15* using a 5 kb genomic fragment. Using expression of the *sec15* cDNA in eyes in an *eyFLP; sec15* background, we rescued both the R7–R8 terminal layering defect and the on and off transients of the ERG (Figure 3D). These data show that phenotypes observed in the mutants are due to loss of Sec15. The identification of mutations in *sec15* in a screen for synaptic specificity defects was unanticipated, given the proposed role of the exocyst in cellular polarization (Nelson, 2003) and neurite outgrowth, as well as the cell lethality associated with the loss of *sec5* in photoreceptors (Murthy et al., 2003).

Sec15 Is Required in Photoreceptors for Synaptic Specificity but Does Not Play an Important Role in Neurotransmitter Release

The *eyFLP* system generates homozygous mutant photoreceptors, as well as homozygous mutant lamina and medulla cells (Lee et al., 2003). This implies that some aspects of the *sec15* mutant phenotype that we observe may not be caused by loss of Sec15 in photoreceptors. Our finding that driving the *sec15* cDNA only in eye tissue largely rescues the R7/R8 targeting defects as well as the ERG defect in *eyFLP; sec15* mutant optic lobes indicates that Sec15 plays a critical role in photoreceptors. To further investigate the cell type-specific aspects of the observed phenotypes, we devised two sets of experiments.

First, we used the *eyFLP* system in combination with the MARCM technique (Lee and Luo, 1999) to generate laminae in which 50% of the photoreceptors are homozygous mutant for *sec15* in a random distribution. In these laminae, mutant photoreceptors express GFP, while other mutant optic lobe cells are not marked. Strong morphological disruptions are invariably and selectively seen in clones with marked mutant photoreceptors (Figures 4A–4C). Interestingly, areas with no mutant photoreceptors have very subtle or no morphological defects. These areas may contain mutant optic lobe cells despite not having any mutant photoreceptor terminals. Since we use an eye-specific driver to express GFP in mutant cells, the lamina cells that are mutant will not be marked. This finding indicates that the contribution of these cells to the overall morphological phenotype is minor. We also observed elevated levels of chaoptin in isolated mutant terminals at the clone borders (Figures 4A–4C). To quantify this effect, we analyzed 12 cartridges at clone boundaries containing single mutant photoreceptor terminals. We made 3D reconstructions of mutant terminals with one adjacent control terminal in each cartridge and calculated pairwise mean fluorescence level ratios between mutant and control terminals. Isolated mutant terminals displayed a 62.3% (±11.7%) increase in chaoptin levels, indicating a cell-autonomous upregulation of chaoptin in *sec15* mutant photoreceptor terminals.

In a second set of experiments, we made use of a new *eyeless* FLPase system developed by Iris Salecker and colleagues, called *ey3.5FLP.* This system uses a specific *eyeless* enhancer that only drives FLPase expression in eye imaginal discs (I. Salecker, personal

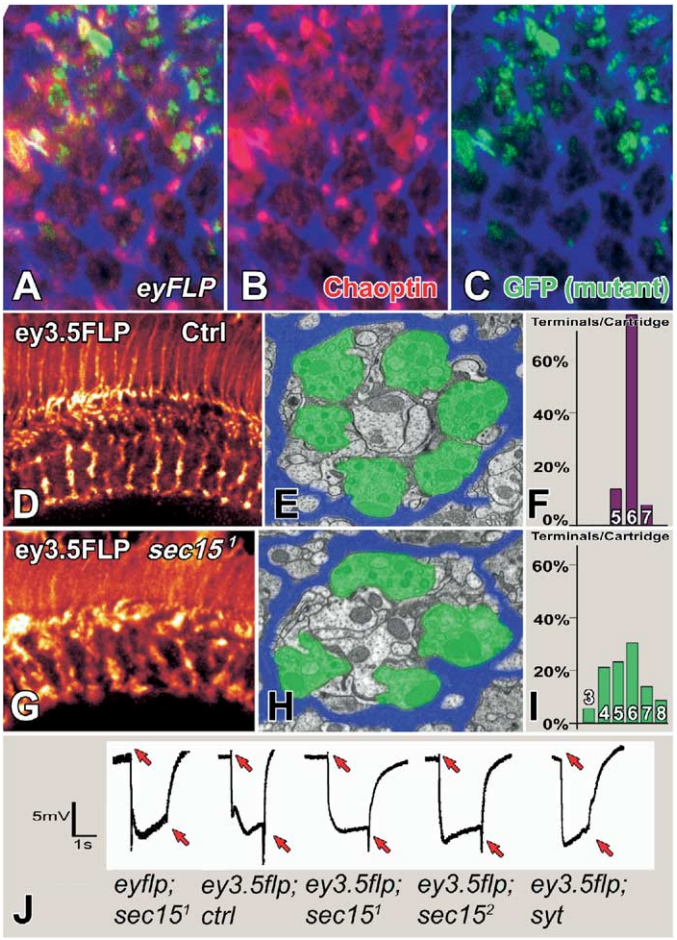

Figure 4. Sec15 Is Required in Photoreceptors for Synaptic Specificity but Not Neurotransmitter Release

(A–C) Lamina of an adult fly of the genotype *eyFLP; GMR-GAL4/UAS-CD8-GFP; FRT sec15[1]/FRT82B tub-GAL80*. This lamina has ~50% control (heterozygous) and 50% homozygous *sec15[1]* mutant photoreceptors. The mutant photoreceptors express GFP (green). Red indicates chaoptin expression (mAb 24B10), and blue shows the outline of the cartridges by marking glial cells (anti-Ebony). Notice that mutant photoreceptors are mis-sorted and express higher levels of chaoptin.

(D) Single optical section taken through the medulla of a fly with the genotype *ey3.5FLP; FRT82B/FRT82cl* stained with mAb24B10. Notice that R7/R8 targeting is normal and not affected by the *ey3.5FLP* system.

(E) TEM of a cartridge from a control (*ey3.5FLP;FRT82B*) lamina with the inset showing outlines of the six photoreceptor terminals in the cartridge.

(F) Distribution of photoreceptor terminals per cartridge for control (*ey3.5FLP;FRT82B*) laminae (n = 66).

(G) Single optical section taken through the medulla of a fly with the genotype *ey3.5FLP; sec15[1]/FRT82cl* stained with mAb24B10. Notice the loss of discrete R7/R8 layers. Compare with Figure 1H to see that the *sec15* mutant phenotype is less severe with the *ey3.5FLP* system compared to the *eyFLP* system.

(H) TEM of a cartridge from a mutant (*ey3.5FLP; FRT sec15[1]/FRT82B cl*) lamina with the inset showing the outlines of the four photoreceptor terminals in the cartridge.

(I) Distribution of photoreceptor terminals per cartridge for mutant (*ey3.5FLP; FRT sec15[1]/FRT82B cl*) laminae (n = 72 cartridges from 5 flies). Notice that the distribution of terminals per cartridge is broader than control (see [F]), but not as broad as mutant laminae generated with the *eyFLP* system (compare to Figure 2D).

(J) Electroretinogram traces. On and off transients are marked with red arrows. *ey3.5FLP* control flies exhibit normal depolarization and on/off transients. Using the *eyFLP* system, *sec15[1]* mutant flies have no on/off transients. However, using the *ey3.5FLP* system, *sec15[1]* mutant flies have small on/off transients. The *ey3.5FLP* system is capable of producing mutant flies that have no on/off transients, using mutations in *syt*, for example.

communication). This ensures that the only mutant terminals in the lamina are from photoreceptors. We found that *ey3.5FLP; sec15* mutant optic lobes still exhibit neuronal targeting defects (Figures 4D and 4G). However, the ERGs exhibit on and off transients, albeit at reduced size (Figure 4J). This clearly indicates that neurotransmitter release persists in photoreceptors lacking Sec15, even though TEM of the laminae of these flies revealed cartridges with abnormal numbers of terminals (Figure 4H). However, the distribution of terminals per cartridge for *sec15* mutants was less broad using the *ey3.5FLP* system compared to the *eyFLP* system (Figure 4I, compare to Figure 2D). These data indicate that Sec15 is required for neuronal targeting in photoreceptors and also serves a function in other neurons. Since on and off transients in ERGs are field potential recordings of the synchronized firing of postsynaptic cells in the lamina, we suspect that the loss of on and off transients in *eyFLP; sec15[1]* flies are secondary to the morphological defects. If only photoreceptors are made mutant using the *ey3.5FLP* system, the miswiring is less severe, causing small on and off responses to return. Likewise, when only nonphotoreceptor optic lobe cells are made mutant in the photoreceptor-specific *sec15* cDNA rescue of the *eyFLP; sec15[1]* phenotype, on and off responses also persist and the R7/R8 targeting defect is greatly reduced (Figure 3D). Sec15 must be removed from both populations of neurons (as in the *eyFLP* system) in order to eliminate the on and off responses, indicating that the loss is a cumulative effect secondary to morphological disruptions. Our data argue that Sec15 is required in photoreceptors for correct neuronal targeting, but does not play an important role in regulating neurotransmission.

Sec15 Is Expressed in Developing Neuropil

To determine the expression pattern and subcellular localization of Sec15, we generated a polyclonal antibody against a fragment of Sec15 (blue box in Figure 3C). The antibody is specific to Sec15, as staining of *sec15* homozygous mutant eye disc clones display a reduction of staining to background levels.

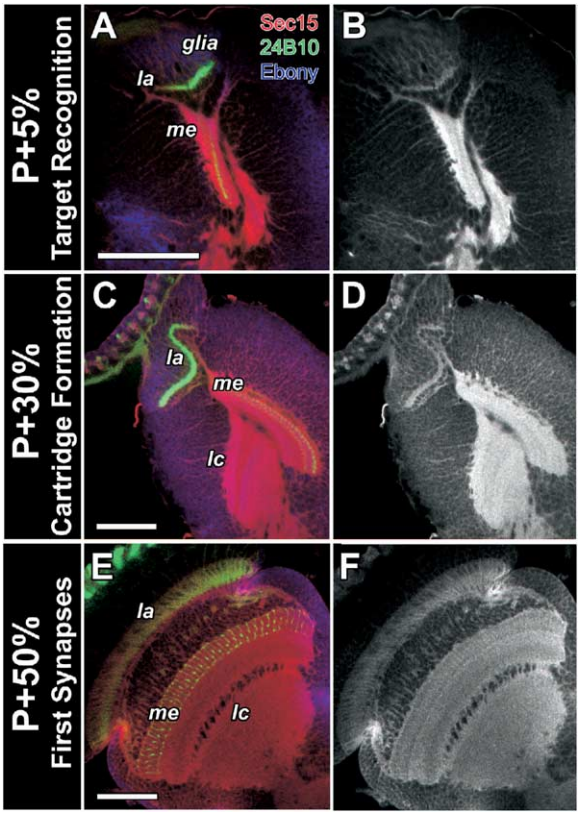

Figure 5. Sec15 Is Expressed in Developing Neuropil

(A) Optic lobe of a wild-type pupa at P + 5% (5% of pupal development) stained with mAb24B10 (green) to mark photoreceptor projections. Anti-Ebony (blue) marks glia, and anti-Sec15 (red) reveals strong immunoreactivity in the developing neuropil. During this stage of development, photoreceptor axons invade the optic lobe and stop at either the developing lamina (la) or medulla (me). (B) Grayscale version of image in (A) showing only Sec15 staining.

(C) Optic lobe of a wild-type pupa at P + 30% stained with the same antibodies as (A). During this stage of development, photoreceptor terminals are being organized into cartridges in the lamina and layers in the medulla. All developing neuropils express Sec15 at high levels. lc, lobula complex. (D) Grayscale version of image in (C) showing only Sec15 staining. (E) Optic lobe of a wild-type pupa at P + 50%; channels as above. (F) Grayscale version of image in (E) showing only Sec15 staining. Notice that the staining intensity is reduced when compared to (B) and (D) in the neuropil. Scale bars are 50 μm in (A) for (A) and (B), (C) for (C) and (D), and (E) for (E) an (F).

During initial target recognition with glia (5% of pupal development) and during cartridge formation (30%), Sec15 immunoreactivity is highly enriched in the developing optic lobe neuropils, including the lamina and medulla (Figure 5). Costaining with mAb24B10 shows that photoreceptor terminals contain Sec15, as do synaptic terminals of other cells that contribute to the neuropil. In the second half of pupation, synapse formation commences in the lamina, and Sec15 immunoreactivity decreases in all neuropils (compare Figure 5F to Figures 5B and 5D). However, low levels of Sec15 immunoreactivity persist into adulthood in a very distinct punctate staining pattern. As shown in Figure S3, Sec15 punctae are localized within the glial border (blue) of each cartridge, indicating that they are present in photoreceptor terminals as well as pre- and postsynaptic endings of other cell types. These punctae mostly do not colocalize with n-synaptobrevin and synaptotagmin I and are located near active zones. In summary, our data indicate that Sec15 is present at the correct time and place during development to account for the neuronal targeting defects in the mutants and may serve other functions into adulthood by specifying distinct subdomains of synaptic terminals.

Specific Cell Adhesion and Signaling Molecules Are Mislocalized in *sec15* Mutant Photoreceptor Terminals

Elevated levels of chaoptin in photoreceptor terminals have been described for another vesicle-trafficking mutant, the vesicle-SNARE *neuronal-synaptobrevin* (*n-syb*). This mutant was also reported to exhibit neuronal targeting defects (Hiesinger et al., 1999). This observation raises the possibility that vesicle-dependent trafficking of transmembrane or other signaling molecules might be responsible for the neuronal targeting defects of *sec15* mutant photoreceptors. Recently, Zhang et al. (2004) identified Rab11 as an interacting partner of Sec15 in mammalian cell culture and proposed that Sec15 is an effector for some but not all Rabs. Indeed, we found an accumulation or upregulation of Rab11 immunoreactivity in *sec15* mutant photoreceptors (S.Q.M., unpublished data), consistent with Rab11-positive vesicles failing to fuse with their target sites. To further test this hypothesis, we examined the localization of cell adhesion and signaling molecules in mutant photoreceptor cell bodies as well as terminals during photoreceptor development, precisely when target selection and cartridge formation occur (between P + 5% to P + 40%). We chose to examine proteins that have either been shown to be required for photoreceptor target selection, such as Dlar (Clandinin et al., 2001; Maurel-Zaffran et al., 2001), N-cadherin (Lee et al., 2001), flamingo (Lee et al., 2003), and IrreC-rst (Schneider et al., 1995), or that are likely to be required, based on work in other systems, such as Armadillo (*Drosophila* β-catenin) (Elul et al., 2003; Yu and Malenka, 2003), chaoptin (Barton et al., 2003), and fasciclin II (Fas2) (Thomas et al., 1997).

We first investigated Fas2 localization in *sec15* mutant photoreceptors, since chaoptin upregulation coincides with elevated levels of Fas2 in *n-syb* mutant photoreceptors (Hiesinger et al., 1999). As shown in Figures 6A–6C, Fas2 appears to be present in aggregates in *sec15* mutant photoreceptor cell bodies at P + 20%, in contrast to wild-type photoreceptors. In addition, the neuronal connections of the cell bodies shown in Figures 6A–6C exhibit Fas2 aggregated along the length of the mutant axons (Figures 6D–6F). Similarly, overexpression of Fas2 in photoreceptors causes neuronal targeting defects between P + 20% and P + 40% (P.R.H., unpublished data). In contrast to *n-syb*, however, no elevated levels of Fas2 are observed later in development. Hence, the data suggest that an aberrant localization of Fas2 in a specific developmental time window may at least partially underlie the observed phenotypes.

Similar mislocalization phenotypes in photoreceptor cell bodies were also observed for other cell adhesion

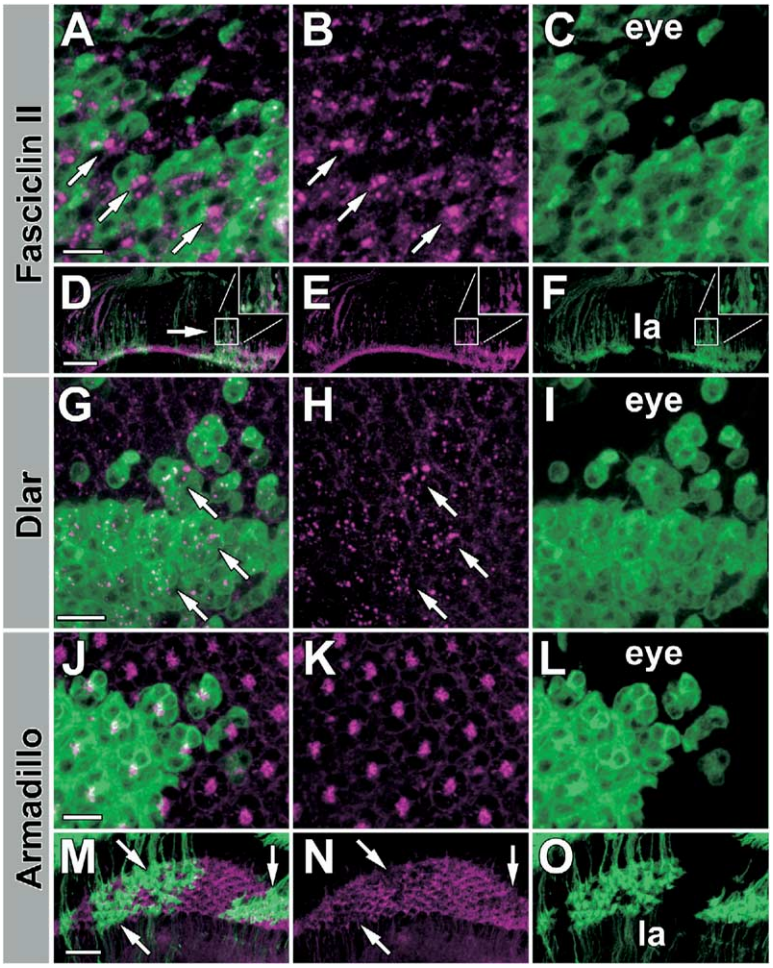

Figure 6. Mislocalization of Cell Adhesion and Signaling Molecules in *sec15* Mutant Photoreceptors

All pupae shown are of the same genotype described in Figure 4A (50% *eyFLP* MARCM). (A–C) P + 15% eye. GFP (green) marks homozygous $sec15^{1}$ mutant photoreceptors. Fas2 aggregates (magenta) only appear in mutant cells. (D–F) Optic lobe of the same animal as in (A)–(C). GFP (green) marks projections of $sec15^{1}$ mutant photoreceptors. The horizontal stripe of Fas2 (purple) is the developing lamina. Notice that aggregates of Fas2 appear only in mutant axons (insets). (G–I) P + 25% eye. GFP (green) again marks homozygous $sec15^{1}$ mutant. Dlar (magenta) exhibits randomly distributed aggregates in mutant photoreceptor cells. (J–L) P + 30% eye. Notice that there is no difference in armadillo (magenta) in wild-type and mutant (green) tissue. (M–O) Optic lobe of the same animal as in (J)–(L). GFP (green) marks projections of mutant photoreceptors. Armadillo is mislocalized in mutant patches. Scale bars for (A)–(C) in (A), 10 μm; for (D)–(F) in (D), 20 μm; for (G)–(I) in (G), 10 μm; for (J)–(L) in (J), 20 μm; for (M)–(O) in (M), 20 μm.

molecules such as Dlar and IrreC-rst during the developmental time window of photoreceptor target selection (Figures 6G–6I and data not shown). Dlar is normally restricted apically in developing wild-type photoreceptors, at the center of the ommatidial array. In *sec15* mutant photoreceptors it appears much more randomly distributed, such that a basal optical section through the eye shows Dlar at higher levels in mutant ommatidia (Figures 6G–6I). Although these results show mislocalization of cell adhesion molecules in the correct cell at the time when they are known to be required for proper target selection, we did not detect obvious defects in the localization of Dlar or IrreC-rst in the developing lamina (data not shown). This leaves open the question of whether mislocalization of Dlar and IrreC-rst beyond the resolution limit of confocal microscopy additionally contributes to the observed targeting defects.

In vertebrates, Lar is known to localize to adherens junctions (Symons et al., 2002). Hence, a possible explanation for the mislocalization of Fas2, IrreC-rst, and Dlar in mutant photoreceptor cell bodies is a defect of adherens junctions. We analyzed the subcellular localization of the adherens junction markers N-cadherin and armadillo in the cell bodies as well as the terminals of mutant photoreceptors, but did not detect any mislocalization of N-cadherin in either compartment. However, armadillo displayed localization defects selectively in the developing lamina, but not the photoreceptor cell bodies (Figure 6J–6O). We also tested several other cell adhesion and signaling molecules, including flamingo (Lee et al., 2003), Slit (Rothberg et al., 1988), Liprin-α (Kaufmann et al., 2002), Crumbs (Izaddoost et al., 2002), and Bazooka (Wodarz et al., 2000), all of which did not display aberrant localization at the level of light microscopy. We conclude that a specific subset of proteins is mislocalized in *sec15* mutants.

Sec15 Is Required for the Localization of Some but Not All Exocyst Members to Neuronal Terminals

Does Sec15 exert an exocyst-dependent function at the neuronal terminal? To date, only one other mutant has been reported that affects a component of the exocyst in *Drosophila*, namely *sec5* (Murthy et al., 2003). Murthy and colleagues showed that Sec5 is required for cell polarization in the developing oocyte and neurite outgrowth in cell culture. In vivo, homozygous mutations in *sec5* are lethal in photoreceptor neurons (Murthy et al., 2003), as are mutations in *sec6* (S.B. and U.T., unpublished data). In contrast, we observe that *sec15* homozygous mutant photoreceptor neurons are viable, even in aged flies (data not shown). Either Sec15

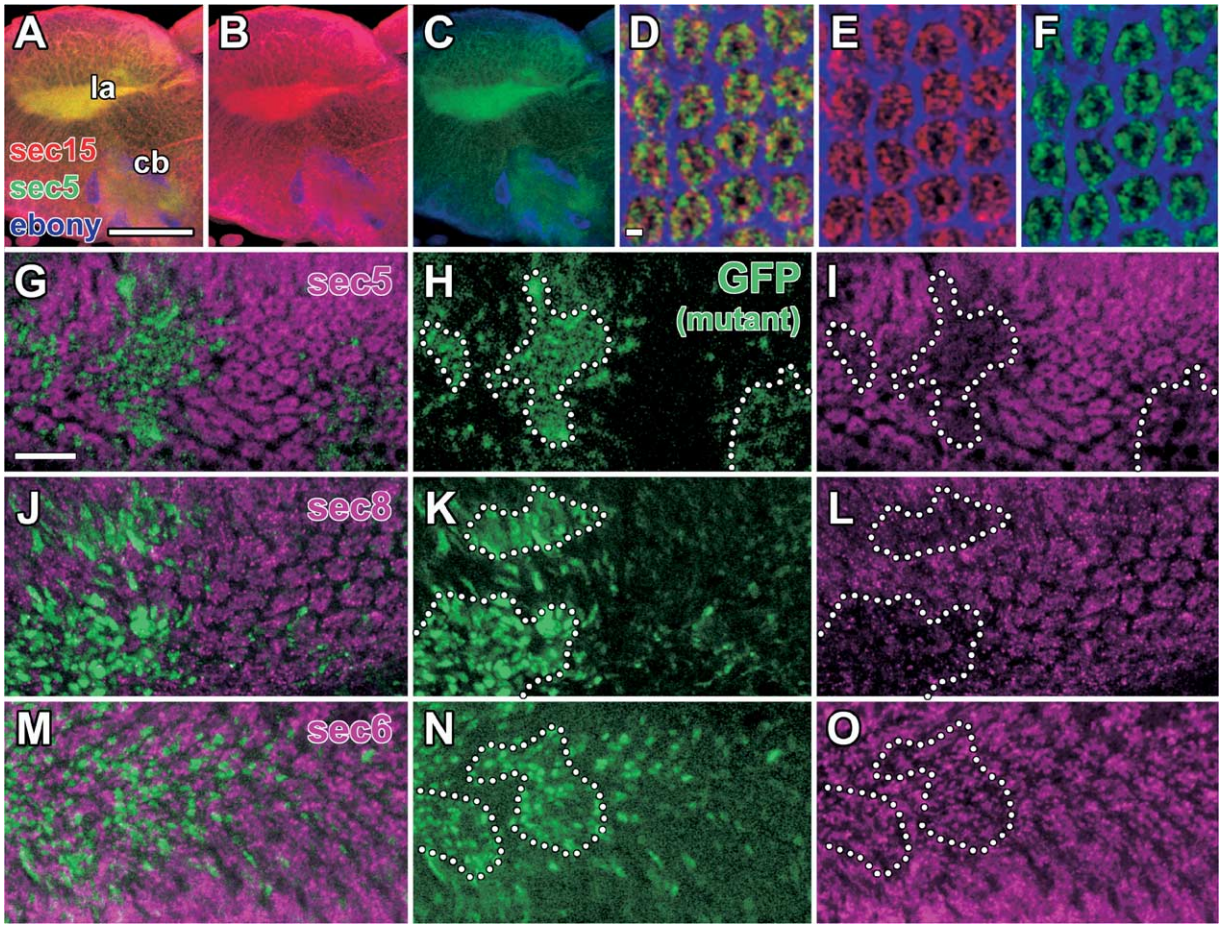

Figure 7. Sec5 and Sec8, but Not Sec6, Localization Depend on Sec15

(A–C) Optic lobe of a wild-type third instar larva stained with anti-Sec15 (red), anti-Sec5 (green), and anti-Ebony (blue). (B) and (C) show the red and green channels of (A) separately. Sec15 and Sec5 are both strongly expressed and colocalize in the developing lamina (la). They are also both expressed in the central brain (cb) of the larva, albeit at lower levels. (D–F) Deconvolved image of an adult wild-type lamina stained with the same antibodies as in (A). Sec15 and Sec5 partially colocalize in photoreceptor terminals, with Sec15 having a more punctate distribution. Anti-Ebony demarcates the outlines of the cartridges.

(G–I) Adult lamina in which approximately 50% of photoreceptor terminals are homozygous mutant for *sec15*^{1} and marked with GFP (green) using the MARCM technique (Lee and Luo, 2001). (H) and (I) show the green and magenta channels of (G) separately. Dashed lines demarcate areas of mutant patches. Sec5 immunoreactivity (magenta) is significantly reduced in homozygous *sec15*^{1} mutant patches. (J–L) Adult lamina of the same genotype as (G–I), but stained with an antibody against Sec8 (magenta). Sec8 staining is also significantly reduced in *sec15*^{1} mutant patches. (M–O) Adult lamina of the same genotype as (G)–(I), but stained with an antibody against Sec6 (magenta). Immunoreactivity levels are the same inside and outside areas with *sec15*^{1} mutant photoreceptor terminals, indicating that Sec15 does not affect Sec6 localization. Scale bars for for (A)–(C) in (A), 50 μm; for (D)–(F) in (D), 2 μm; for (G)–(O) in (G), 10 μm.

exerts a function independent of the exocyst at the neuronal terminal, or its developmental role only represents a specialized task of the complex or subcomplex. To distinguish between these two possibilities, we investigated the localization of Sec5, Sec6, and Sec8 in developing neuropil as well as in *sec15* mutant clones.

In the developing lamina of the late third instar larva, Sec5 and Sec15 colocalize (Figures 7A–7C). Both are highly enriched in the developing neuropil, whereas immunoreactivity in the functional larval central brain is much lower (Figures 7A–7C, cb). In the adult lamina, Sec5 and Sec15 are coexpressed in cartridges. Sec5 colocalizes with Sec15 to a larger extent than any of the other markers tested, including plasmalemmal, synaptic vesicle, or active zone markers (Figures 7D–7F and Figure S4). However, the colocalization of Sec15 and Sec5 is not perfect, leaving subdomains marked only by anti-Sec15 or anti-Sec5. These data suggest that Sec5 and Sec15 may have common as well as separate functions.

We subsequently tested the expression patterns of two other presumed core members of the exocyst, Sec6 and Sec8, using two newly generated polyclonal antibodies (see Experimental Procedures). In adult lamina cartridges, Sec6 immunoreactivity exhibits a very specific pattern that exactly matches the localization of the postsynaptic lamina monopolar cells (cf. Figures S4A–S4D and Figure 1D). In contrast, the antibody against Sec8 exhibits a punctate staining pattern throughout the cartridges that is similar to Sec15 (Fig-

ures S4E–S4H). Likewise, Sec6 and Sec8 antibodies have both specific but different staining patterns in the developing brain: Sec6 strongly colocalizes with Sec5 in developing neuropil, whereas Sec8 is enriched in cell bodies but is almost completely excluded from the developing neuropil (Figures S4I–S4N). Finally, we performed stainings to examine the localization of Sec15, Sec6, and Sec8 at the third instar larval neuromuscular junction. As shown in Figure S5, Sec15 is present in both boutons and muscle cells, but seems enriched at boutons. In contrast, Sec 6 is highly enriched at the Z bands of muscle cells and very weakly present in boutons, while Sec8 is not present in muscle cells or neurons, but is in a highly punctate distribution in unidentified processes that may be glial projections. These data are not consistent with a single functional Sec6/8 complex.

To test whether Sec15 at the photoreceptor terminals affects Sec5, Sec6, and Sec8, we investigated the presence of these proteins in *sec15* mutant clones. As shown in Figures 7G–7I, Sec5 immunoreactivity in *sec15* mutant clones of photoreceptor terminals in the lamina is markedly reduced and possibly absent in the terminals. Likewise, Sec8 immunoreactivity is reduced in *sec15* mutant clones of photoreceptor terminals (Figures 7J–7L). However, the levels of Sec6 appear to be unaffected by mutations in *sec15* (Figures 7M–7O). This is likely because Sec6 is enriched in postsynaptic cells in the lamina (Figure S4) and because it seems to be absent presynaptically. In addition, the specific developmental and adult staining patterns of Sec8 (Figures S4 and S5), as well as its downregulation in *sec15* mutant clones, suggest common and separable functions compared to *sec5*, *sec6*, and *sec15* at different points in development. Since loss of *sec5* in photoreceptors causes cell lethality, the loss or downregulation of Sec5 in *sec15* mutant terminals is unlikely to reflect a global loss of the protein. Our data rather suggest that Sec15 is required for localization of Sec5 and Sec8, but not Sec6 to the presynaptic photoreceptor terminal. These data suggest that Sec15 may recruit or stabilize a complex that includes some but not all exocyst members in photoreceptor terminals in a spatiotemporally regulated manner.

Discussion

Here we present evidence that the *Drosophila* homolog of Sec15 plays a specific role in synaptic targeting and that loss of the protein causes phenotypes that differ significantly from the phenotypes associated with the loss of Sec5. Our data indicate that Sec15 is required for the subcellular distribution and delivery of a specific subset of proteins and that there are separable functions of individual exocyst components in flies.

Specific Functions of Exocyst Components in Neurons

It is surprising how many developmental processes are unaffected by the loss of *sec15*: neuronal differentiation, axonal outgrowth, and initial target recognition of the correct brain areas all appear normal. Subsequently, a specific neuronal sorting process that ensures synaptic specificity is disrupted. After the defective neuronal targeting step, the developmental program proceeds rather normally with synaptic partner selection and synapse formation. While it is known that these developmental processes are genetically separable (Lee et al., 2003; P.R.H., unpublished data), they have primarily been associated with cell adhesion molecules (CAMs). Based on our finding of targeting defects for specific CAMs and signaling molecules, we propose that a vesicular transport mechanism exists to spatiotemporally target certain CAMs as well as other proteins. Notably, soluble NSF-attachment receptors (SNAREs), which are required for most if not all vesicle docking and fusion processes, are unlikely to convey much spatiotemporal targeting information. This is primarily because target-SNAREs are distributed uniformly over membranes, even though vesicle fusion is restricted to limited subdomains (reviewed in Guo et al., 2000), as is also the case for the target-SNARE syntaxin in photoreceptor terminals (Hiesinger et al., 2001).

Further evidence for targeting defects of a vesicular cargo transport mechanism comes from vertebrate cell culture experiments. Grindstaff and colleagues showed that disrupting exocyst function caused defects in basolateral, but not apical, targeting of proteins in epithelial cells (Grindstaff et al., 1998). The exocyst has also been implicated in the trafficking of GLUT4 transporters in response to insulin stimulation (Inoue et al., 2003). Sans and colleagues showed that Sec8 is involved in NMDA receptor insertion at dendrites through an interaction with SAP102 (Sans et al., 2003). In *Drosophila* photoreceptors, the basolateral compartment is the axon (Izaddoost et al., 2002), while in vertebrate neurons, the basolateral compartment is dendritic (Winckler and Mellman, 1999). It is therefore possible that the same subcomplex of exocyst (and other) components is required for correct targeting in the presynaptic compartment of *Drosophila* photoreceptors and vertebrate postsynaptic receptor targeting.

Vesicle Trafficking and Synaptic Specificity

The investigation of the establishment of specific synaptic contacts has largely been focused on CAMs and their regulating/modifying proteins, since these molecules are thought to convey information about spatiotemporal specificity (Clandinin and Zipursky, 2002). The finding of CAM misregulation in *sec15* mutant neurons links the spatiotemporal regulation of CAMs to the cell biology of the neuron. Although we have not examined vesicle trafficking of CAMs directly, recent work in both yeast and vertebrate systems provides evidence that Sec15 and other exocyst members are associated with vesicles and play a role in vesicle trafficking (Ang et al., 2004; Boyd et al., 2004). We propose that specificity may be established through unique vesicular trafficking mechanisms in addition to the transcriptional and post-translational regulation of various isoforms of CAMs in certain cells at distinct times. Much is known about the specificity of the vesicular trafficking machinery at the ER and Golgi, where distinct cargoes need to be specifically targeted (Duden, 2003; Spang, 2004). In neurons, numerous synaptic proteins, including the CAM N-cadherin are specifically targeted to the active zones and

other synaptic domains via a specialized vesicular transport mechanism (Zhai et al., 2001). In *Drosophila* photoreceptors, the misregulation of CAMs prior to synapse formation has been previously observed in neurons that lack n-synaptobrevin (Hiesinger et al., 1999), and specific vesicles for the targeted transport of synaptic components have been described in mammals (Zhai et al., 2001). It is not known whether a distinct type of vesicle exists for the transport of CAMs and signaling molecules to the developing terminal, but we propose that specific subsets of CAMs are transported and integrated into the membrane by Sec15. This is not to say that synaptic specificity is the only role of Sec15 or the CAMs we have examined. Our data shows mislocalization of CAMs in both the cell body as well as axons of *sec15* mutant photoreceptors. We have not investigated the consequences of this cell body mislocalization, except to make sure that it does not impact cell viability, neuronal differentiation, axonal outgrowth, and initial target recognition of the correct brain areas by these photoreceptors. In this respect, it is interesting to note that some of the CAMs we examined (N-cadherin, flamingo) were correctly targeted in mutant photoreceptors while others (Dlar, Fas2, IrreC-rst) were not. Although the in vitro inhibition of microtubule polymerization by exocyst members (Wang et al., 2004) and defects in *sec5* mutants (Murthy et al., 2003) with neurite extension may argue for a role in general protein or membrane trafficking for the exocyst, our data argue that this is not the case for Sec15. In addition to the correct localization of the CAMs mentioned above, *sec15* mutant neurons are viable, extend axons, and assemble functional synapses. It seems unlikely that a loss of protein required for general protein trafficking would not affect these processes. In summary, our data describe a defect in synaptic specificity and concommitant mislocalization of proteins known to affect synaptic specificity in photoreceptors lacking Sec15. These defects can be explained by a Sec15-dependent intracellular vesicle trafficking mechanism for certain molecular components that are required for the establishment of synaptic specificity.

The Exocyst: One Complex or Subcomplexes with Multiple Functions?

Most studies consider individual exocyst components representative for the whole complex and assume that the entire eight member complex is responsible for the different roles proposed or demonstrated for the exocyst (Finger and Novick, 1998; Grindstaff et al., 1998; Guo et al., 1999; Hazuka et al., 1999; Hsu et al., 1999; Murthy et al., 2003). As we isolated mutations in *sec15*, *Drosophila* was the first metazoan in which two independent gene disruptions of exocyst components allowed us to test this assumption. Furthermore, a gene disruption of *Drosophila sec6* has recently been generated and, like *sec5*, observed to cause cell lethality in homozygous mutant eyes (S.B. and U.T., unpublished data). The remarkable difference between *sec5*, *sec6*, and *sec15* mutant phenotypes questions the idea of a mutation in an individual member having a "generic exocyst" phenotype. One possibility that may explain this discrepancy would be an exocyst-independent function of *sec15*. Our findings that Sec5 and Sec8 are mislocalized in *sec15* mutant neuronal terminals argue against this possibility. Instead, it suggests that Sec15 participates with Sec5 and Sec8 in a specific developmental process. However, the *sec15* phenotype is notably more specific than the *sec5* or *sec6* cell lethality. While Sec5 is suggested to have a role in general membrane trafficking (Murthy et al., 2003), the large number of normal processes we observe in *sec15* mutant neurons (cell viability, axon outgrowth, axon guidance, neurotransmitter release, etc.) argues against this being the case for Sec15. This implies that at least Sec5 and perhaps Sec8 sustain another essential function in the absence of Sec15. For the Sec15 interaction partner Sec10, a knockdown using RNAi as well as Sec10 overexpression were found to have no detectable phenotype in photoreceptors (Andrews et al., 2002). However, Sec10 overexpression in *sec15* mutant photoreceptors causes cell lethality (S.Q.M., unpublished data), indicating a genetic interaction. Moreover, the finding that Sec6 is normally localized in the absence of Sec15 is puzzling. Close investigation of the expression pattern in lamina cartridges revealed a clear postsynaptic localization of Sec6. This finding together with the differential expression patterns of Sec5, Sec6, Sec8, and Sec15 during development and adulthood argue against a single functional complex in *Drosophila* neurons. Similarly, immuno-EM in rat hippocampal neurons revealed that Sec6 localizes to secretory vesicles, while Sec8 has a diffuse, cytoplasmic distribution (Vik-Mo et al., 2003). Another precedent for subcomplexes of the exocyst having different functions can be found in the COG complex. The COG, exocyst, and GARP complexes share distant homology in the N termini of their subunits and are placed in a family of "quatrefoil complexes" by Munro and colleagues because all three complexes have multiples of four subunits (Whyte and Munro, 2001). Distinct COG subcomplexes are proposed to act in intra-Golgi vesicle recycling and endosome to Golgi recycling (Whyte and Munro, 2002). A similar situation may exist for the exocyst, where subcomplexes are involved in trafficking different populations of vesicles. Although we do not know which assemblies of exocyst components exert which functions in vivo, our results suggest that at least two different functional compositions of the known exocyst components exist. Given that Sec5 is considered the core member of the complex (Guo et al., 1999), loss of *sec5* may represent either the loss of all exocyst functions as suggested by Murthy et al. (2003), or of at least one essential function. Either way, the cell lethality associated with the loss of *sec5* or *sec6* masks possible later more specific functions of subcomplexes. Hence, our data indicate that a detailed analysis of the many proteins that are thought to be required for exocyst function will have to be initiated in order to understand their precise role in metazoans.

Experimental Procedures

Molecular Biology and Antibody Production

sec15^{1} and *sec15*^{2} alleles were sequenced in *trans* to an isogenized chromosome using standard techniques (Zhai et al., 2003). See Supplemental Experimental Procedures for details concerning

rescue constructs. Antibody production: the cDNA sequence corresponding to amino acids 382–697 of Sec15 was cloned into the pET28a (Invitrogen) vector for protein expression (gift of S. Wu). The cDNA fragment was cloned into BamHI and NotI restriction sites using PCR primers that introduced those sites into the cDNA fragment as described for the cDNA rescue construct. Guinea pig antibodies against this domain were raised by Cocalico Biologicals (Reamstown, PA) using the purified recombinant protein. Antisera against the full-length Sec15 protein were also raised in this manner. Although the antisera to the full-length protein did not recognize truncated protein products in the mutants, we cannot exclude the possibility that these anti-sera do not recognize epitopes in putative truncated Sec15 proteins. However, we stress that this possibility is unlikely. Antibodies against Sec6 and Sec8 were generated as follows: a 500 nucleotide fragment of *sec6* (CG5341) and a 750 nucleotide fragment of *sec8* (CG2095) were PCR amplified from genomic DNA and subcloned into pRSETC (Invitrogen) via primer-added BamHI and EcoRI restriction sites. The resulting protein fragments correspond to amino acids 341–507 of Sec6 and amino acids 137–386 of Sec8. Proteins were expressed in BL21 cells, purified on His-columns, and resuspended. Polyclonal antibodies were generated by injecting guinea pigs with 100 mg of protein in Freund's complete adjuvant, followed by three boosts of 75 mg, 35 mg, and 35 mg of protein in incomplete Freund's adjuvant at 3 week intervals. All three antibodies recognized the appropriate-sized band on Western blot (data not shown). Antibody specificity was confirmed by loss of staining in mutant clonal tissue for anti-Sec15 (Figure S6) as well as loss of the bands of the appropriate sizes on Western blots of mutant tissue for both anti-Sec15 and anti-Sec6 (data not shown). The loss of Sec15 staining in mutant clonal tissue from third instar eye discs (Figure S6) also argues that there is no perdurance of Sec15 protein in mutant photoreceptors at the time of axon outgrowth and establishment of synaptic specificity. However, we must note that the possibility of minute amounts of perdurance cannot completely be excluded. Anti-Sec8 recognized overexpressed Sec8 protein in tissue (Figure S7), but was not tested on *sec8* mutants, as none were available.

Mosaic Analyses

See Supplemental Experimental Procedures.

ERGs and Phototaxis Assays

Electroretinograms and phototaxis assays were performed as described previously (Verstreken et al., 2003).

Transmission Electron Microscopy

TEM was performed as described previously (Verstreken et al., 2003). The laminae examined are from *y w eyFLP;;sec15*^{1} or *sec15*^{2} or *FRT82B*^{isogenized}*/FRT82B cl* animals. For photoreceptor terminal distribution, photoreceptor terminals were identified by the presence of capitate projections (Meinertzhagen and Hanson, 1993). Cartridges (129) were scored for wild-type laminae (three animals), 75 cartridges were scored for *sec15*^{1} laminae (three animals), and 29 cartridges were scored for *sec15*^{2} laminae (one animal). For synapse quantification, T bars were used to identify synapses, and only those T bars residing within photoreceptor terminals were counted.

Immunocytochemistry, Image Acquisition, and Processing

See Supplemental Experimental Procedures.

Supplemental Data

The Supplemental Data for this article can be found online at http://www.neuron.org/cgi/content/full/46/2/219/DC1/.

Acknowledgments

We would like to thank S. Carroll, K. Cho, A. Hofbauer, G. Mardon, T.L. Schwarz, T. Uemura, D. Van Vactor, A. Wodarz, S. Wu, S.L. Zipursky, the Bloomington Stock Center, and the University of Iowa Developmental Studies Hybridoma Bank for reagents. We especially thank Iris Salecker for making the ey3.5FLP system available to us prior to publication. We would also like to thank H. Andrews, M. Acar, and H. Jafar-Nejad for critical reading of the manuscript and Bellen lab members for comments and discussion. S.Q.M. is supported by NIH grants EY07001 and MH62639 and is a member of the Medical Scientist Training Program. P.R.H., R.G.Z., K.L.S., and H.J.B. are supported by the HHMI. P.R.H. was further supported by an EMBO long-term fellowship. S.B. is supported by a Vision Science Research Program fellowship. This work was also supported by NIH grant MH62639 (to M.C.C.). H.J.B. is an HHMI Investigator.

Received: July 15, 2004
Revised: October 26, 2004
Accepted: February 25, 2005
Published: April 20, 2005

References

Andrews, H.K., Zhang, Y.Q., Trotta, N., and Broadie, K. (2002). Drosophila Sec10 is required for hormone secretion but not general exocytosis or neurotransmission. Traffic *3*, 906–921.

Ang, A.L., Taguchi, T., Francis, S., Folsch, H., Murrells, L.J., Pypaert, M., Warren, G., and Mellman, I. (2004). Recycling endosomes can serve as intermediates during transport from the Golgi to the plasma membrane of MDCK cells. J. Cell Biol. *167*, 531–543.

Barton, W.A., Liu, B.P., Tzvetkova, D., Jeffrey, P.D., Fournier, A.E., Sah, D., Cate, R., Strittmatter, S.M., and Nikolov, D.B. (2003). Structure and axon outgrowth inhibitor binding of the Nogo-66 receptor and related proteins. EMBO J. *22*, 3291–3302.

Bennett, M.K., and Scheller, R.H. (1993). The molecular machinery for secretion is conserved from yeast to neurons. Proc. Natl. Acad. Sci. USA *90*, 2559–2563.

Benzer, S. (1967). Behavioral mutants of *Drosophila* isolated by countercurrent distribution. Proc. Natl. Acad. Sci. USA *58*, 1112–1119.

Boyd, C., Hughes, T., Pypaert, M., and Novick, P. (2004). Vesicles carry most exocyst subunits to exocytic sites marked by the remaining two subunits, Sec3p and Exo70p. J. Cell Biol. *167*, 889–901.

Burg, M., Sarthy, P., Koliantz, G., and Pak, W. (1993). Genetic and molecular identification of a Drosophila histidine decarboxylase gene required in photoreceptor transmitter synthesis. EMBO J. *12*, 911–919.

Clandinin, T.R., and Zipursky, S.L. (2000). Afferent growth cone interactions control synaptic specificity in the Drosophila visual system. Neuron *28*, 427–436.

Clandinin, T.R., and Zipursky, S.L. (2002). Making connections in the fly visual system. Neuron *35*, 827–841.

Clandinin, T.R., Lee, C.-H., Herman, T., Lee, R.C., Yang, A.Y., Ovasapyan, S., and Zipursky, S.L. (2001). Drosophila LAR Regulates R1–R6 and R7 Target Specificity in the Visual System. Neuron *32*, 237–248.

Duden, R. (2003). ER-to-Golgi transport: COP I and COP II function (Review). Mol. Membr. Biol. *20*, 197–207.

Elul, T.M., Kimes, N.E., Kohwi, M., and Reichardt, L.F. (2003). N- and C-terminal domains of beta-catenin, respectively, are required to initiate and shape axon arbors of retinal ganglion cells in vivo. J. Neurosci. *23*, 6567–6575.

Finger, F.P., and Novick, P. (1998). Spatial regulation of exocytosis: lessons from yeast. J. Cell Biol. *142*, 609–612.

Fischbach, K., and Dittrich, A. (1989). The optic lobe of Drosophila melanogaster. I. A golgi analysis of wild-type structure. Cell Tissue Res. *258*, 441–475.

Friedrich, G.A., Hildebrand, J.D., and Soriano, P. (1997). The secretory protein Sec8 is required for paraxial mesoderm formation in the mouse. Dev. Biol. *192*, 364–374.

Frohlich, A., and Meinertzhagen, I.A. (1983). Quantitative features of synapse formation in the fly's visual system. I. The presynaptic photoreceptor terminal. J. Neurosci. *3*, 2336–2349.

Fujita, S., Zipursky, S., Benzer, S., Ferrus, A., and Shotwell, S. (1982). Monoclonal antibodies against the *Drosophila* nervous system. Proc. Natl. Acad. Sci. USA *79*, 7929–7933.

Grindstaff, K.K., Yeaman, C., Anandasabapathy, N., Hsu, S.C., Rodriguez-Boulan, E., Scheller, R.H., and Nelson, W.J. (1998). Sec6/8 complex is recruited to cell-cell contacts and specifies transport vesicle delivery to the basal-lateral membrane in epithelial cells. Cell *93*, 731–740.

Guo, W., Roth, D., Walch-Solimena, C., and Novick, P. (1999). The exocyst is an effector for Sec4p, targeting secretory vesicles to sites of exocytosis. EMBO J. *18*, 1071–1080.

Guo, W., Sacher, M., Barrowman, J., Ferro-Novick, S., and Novick, P. (2000). Protein complexes in transport vesicle targeting. Trends Cell Biol. *10*, 251–255.

Hazuka, C.D., Foletti, D.L., Hsu, S.-C., Kee, Y., Hopf, F.W., and Scheller, R.H. (1999). The sec6/8 complex is located at neurite outgrowth and axonal synapse-assembly domains. J. Neurosci. *19*, 1324–1334.

Hiesinger, P.R., Reiter, C., Schau, H., and Fischbach, K.F. (1999). Neuropil pattern formation and regulation of cell adhesion molecules in Drosophila optic lobe development depend on synaptobrevin. J. Neurosci. *19*, 7548–7556.

Hiesinger, P.R., Scholz, M., Meinertzhagen, I.A., Fischbach, K.F., and Obermayer, K. (2001). Visualization of synaptic markers in the optic neuropils of Drosophila using a new constrained deconvolution method. J. Comp. Neurol. *429*, 277–288.

Hsu, S.C., Ting, A.E., Hazuka, C.D., Davanger, S., Kenny, J.W., Kee, Y., and Scheller, R.H. (1996). The mammalian brain rsec6/8 complex. Neuron *17*, 1209–1219.

Hsu, S.-C., Hazuka, C.D., Foletti, D.L., and Scheller, R.H. (1999). Targeting vesicles to specific sites on the plasma membrane: the role of the sec6/8 complex. Trends Cell Biol. *9*, 150–153.

Hsu, S.C., TerBush, D., Abraham, M., and Guo, W. (2004). The exocyst complex in polarized exocytosis. Int. Rev. Cytol. *233*, 243–265.

Inoue, M., Chang, L., Hwang, J., Chiang, S.H., and Saltiel, A.R. (2003). The exocyst complex is required for targeting of Glut4 to the plasma membrane by insulin. Nature *422*, 629–633.

Izaddoost, S., Nam, S.C., Bhat, M.A., Bellen, H.J., and Choi, K.W. (2002). Drosophila Crumbs is a positional cue in photoreceptor adherens junctions and rhabdomeres. Nature *416*, 178–183.

Kaufmann, N., DeProto, J., Ranjan, R., Wan, H., and Van Vactor, D. (2002). Drosophila liprin-alpha and the receptor phosphatase Dlar control synapse morphogenesis. Neuron *34*, 27–38.

Kee, Y., Yoo, J.-S., Hazuka, C.D., Peterson, K.E., Hsu, S.-C., and Scheller, R.H. (1997). Subunit structure of the mammalian exocyst complex. Proc. Natl. Acad. Sci. USA *94*, 14438–14443.

Kirschfeld, K. (1967). Exp. Brain Res. *3*, 248–270.

Lee, T., and Luo, L. (1999). Mosaic analysis with a repressible cell marker for studies of gene function in neuronal morphogenesis. Neuron *22*, 451–461.

Lee, T., and Luo, L. (2001). Mosaic analysis with a repressible cell marker (MARCM) for Drosophila neural development. Trends Neurosci. *24*, 251–254.

Lee, C.H., Herman, T., Clandinin, T.R., Lee, R., and Zipursky, S.L. (2001). N-cadherin regulates target specificity in the Drosophila visual system. Neuron *30*, 437–450.

Lee, R.C., Clandinin, T.R., Lee, C.-H., Chen, P.-L., Meinertzhagen, I.A., and Zipursky, S.L. (2003). The protocadherin Flamingo is required for axon target selection in the Drosophila visual system. Nat. Neurosci. *6*, 557–563.

Maurel-Zaffran, C., Suzuki, T., Gahmon, G., Treisman, J.E., and Dickson, B.J. (2001). Cell-autonomous and -nonautonomous functions of LAR in R7 photoreceptor axon targeting. Neuron *32*, 225–235.

Meinertzhagen, I.A., and Hanson, T.E. (1993). The development of the optic lobe. In The Development of *Drosophila Melanogaster*, M. Bate and A. Martinez-Arias, eds. (Cold Spring Harbor, NY: Cold Spring Harbor Press), pp. 1363–1491.

Murthy, M., and Schwarz, T.L. (2004). The exocyst component Sec5 is required for membrane traffic and polarity in the Drosophila ovary. Development *131*, 377–388.

Murthy, M., Garza, D., Scheller, R.H., and Schwarz, T.L. (2003). Mutations in the exocyst component Sec5 disrupt neuronal membrane traffic, but neurotransmitter release persists. Neuron *37*, 433–447.

Nelson, W.J. (2003). Adaptation of core mechanisms to generate cell polarity. Nature *422*, 766–774.

Newsome, T.P., Asling, B., and Dickson, B.J. (2000). Analysis of *Drosophila* photoreceptor axon guidance in eye-specific mosaics. Development *127*, 851–860.

Novick, P., Field, C., and Schekman, R. (1980). Identification of 23 complementation groups required for post-translational events in the yeast secretory pathway. Cell *21*, 205–215.

Poeck, B., Fischer, S., Gunning, D., Zipursky, S.L., and Salecker, I. (2001). Glial cells mediate target layer selection of retinal axons in the developing visual system of Drosophila. Neuron *29*, 99–113.

Rothberg, J.M., Hartley, D.A., Walther, Z., and Artavanis-Tsakonas, S. (1988). slit: an EGF-homologous locus of D. melanogaster involved in the development of the embryonic central nervous system. Cell *55*, 1047–1059.

Sans, N., Prybylowski, K., Petralia, R.S., Chang, K., Wang, Y.-X., Racca, C., Vicini, S., and Wenthold, R.J. (2003). NMDA receptor trafficking through an interaction between PDZ proteins and the exocyst complex. Nat. Cell Biol. *5*, 520–530.

Schekman, R., and Novick, P. (2004). 23 genes, 23 years later. Cell *116*, S13–15.

Schneider, T., Reiter, C., Eule, E., Bader, B., Lichte, B., Nie, Z., Schimansky, T., Ramos, R.G., and Fischbach, K.F. (1995). Restricted expression of the irreC-rst protein is required for normal axonal projections of columnar visual neurons. Neuron *15*, 259–271.

Spang, A. (2004). Vesicle transport: a close collaboration of Rabs and effectors. Curr. Biol. *14*, R33–R34.

Stark, W.S., Sapp, R., and Carlson, S.D. (1989). Ultrastructure of the ocellar visual system in normal and mutant Drosophila melanogaster. J. Neurogenet. *5*, 127–153.

Stowers, R.S., and Schwarz, T.L. (1999). A genetic method for generating Drosophila eyes composed exclusively of mitotic clones of a single genotype. Genetics *152*, 1631–1639.

Symons, J.R., LeVea, C.M., and Mooney, R.A. (2002). Expression of the leucocyte common antigen-related (LAR) tyrosine phosphatase is regulated by cell density through functional E-cadherin complexes. Biochem. J. *365*, 513–519.

TerBush, D., Maurice, T., Roth, D., and Novick, P. (1996). The Exocyst is a multiprotein complex required for exocytosis in Saccharomyces cerevisiae. EMBO J. *15*, 6483–6494.

Thomas, U., Kim, E., Kuhlendahl, S., Koh, Y.H., Gundelfinger, E.D., Sheng, M., Garner, C.C., and Budnik, V. (1997). Synaptic clustering of the cell adhesion molecule fasciclin II by discs-large and its role in the regulation of presynaptic structure. Neuron *19*, 787–799.

Vega, I.E., and Hsu, S.-C. (2001). The exocyst complex associates with microtubules to mediate vesicle targeting and neurite outgrowth. J. Neurosci. *21*, 3839–3848.

Verstreken, P., Koh, T.W., Schulze, K.L., Zhai, R.G., Hiesinger, P.R., Zhou, Y., Mehta, S.Q., Cao, Y., Roos, J., and Bellen, H.J. (2003). Synaptojanin is recruited by endophilin to promote synaptic vesicle uncoating. Neuron *40*, 733–748.

Vik-Mo, E.O., Oltedal, L., Hoivik, E.A., Kleivdal, H., Eidet, J., and Davanger, S. (2003). Sec6 is localized to the plasma membrane of mature synaptic terminals and is transported with Secretogranin II-containing vesicles. Neuroscience *119*, 73–85.

Wang, S., Liu, Y., Adamson, C.L., Valdez, G., Guo, W., and Hsu, S.C. (2004). The mammalian exocyst, a complex required for exocytosis, inhibits tubulin polymerization. J. Biol. Chem. *279*, 35958–35966.

Whyte, J.R., and Munro, S. (2001). The Sec34/35 Golgi transport complex is related to the exocyst, defining a family of complexes involved in multiple steps of membrane traffic. Dev. Cell *1*, 527–537.

Whyte, J.R., and Munro, S. (2002). Vesicle tethering complexes in membrane traffic. J. Cell Sci. *115*, 2627–2637.

Winckler, B., and Mellman, I. (1999). Neuronal polarity: controlling the sorting and diffusion of membrane components. Neuron *23*, 637–640.

Wodarz, A., Ramrath, A., Grimm, A., and Knust, E. (2000). Drosophila atypical protein kinase C associates with Bazooka and controls polarity of epithelia and neuroblasts. J. Cell Biol. *150*, 1361–1374.

Yeaman, C., Grindstaff, K.K., and Nelson, W.J. (2004). Mechanism of recruiting Sec6/8 (exocyst) complex to the apical junctional complex during polarization of epithelial cells. J. Cell Sci. *117*, 559–570.

Yu, X., and Malenka, R.C. (2003). Beta-catenin is critical for dendritic morphogenesis. Nat. Neurosci. *6*, 1169–1177.

Zhai, R.G., Vardinon-Friedman, H., Cases-Langhoff, C., Becker, B., Gundelfinger, E.D., Ziv, N.E., and Garner, C.C. (2001). Assembling the presynaptic active zone: a characterization of an active one precursor vesicle. Neuron *29*, 131–143.

Zhai, R.G., Hiesinger, P.R., Koh, T.W., Verstreken, P., Schulze, K.L., Cao, Y., Jafar-Nejad, H., Norga, K.K., Pan, H., Bayat, V., et al. (2003). Mapping Drosophila mutations with molecularly defined P element insertions. Proc. Natl. Acad. Sci. USA *100*, 10860–10865.

Zhang, X.M., Ellis, S., Sriratana, A., Mitchell, C.A., and Rowe, T. (2004). Sec15 Is an Effector for the Rab11 GTPase in Mammalian Cells. J. Biol. Chem. *279*, 43027–43034.